J MATER RES TECHNOL. 2020;9(3):6950–6956

Available online at www.sciencedirect.com

jmr&t
Journal of Materials Research and Technology
www.jmrt.com.br

Short Communication

Creating *in-situ* alloys by welding — new perspectives for advanced materials and applications

Marcelo F. Motta[a], *Kamilla G. Santiago*[b], *Edson F. Pessoa*[c], *Ana C. Rodrigues*[a], *Igor P. Fernandes*[a], *Hélio C. de Miranda*[a], *Cleiton C. Silva*[a,*]

[a] *Universidade Federal do Ceará, Department of Metallurgical and Materials Engineering, Welding Research and Technology Laboratory, 60455-760, Fortaleza, Ceará, Brazil*
[b] *Instituto Federal de Educação, Ciência e Tecnologia do Ceará — Campus Horizonte, Francisca Cecilia de Sousa Street, Planalto Horizonte, 62884-105, Horizonte, Ceará, Brazil*
[c] *Instituto Federal de Educação, Ciência e Tecnologia do Ceará – Campus Caucaia, Francisco da Rocha Martins Avenue, Pabussu, 61609-090, Caucaia, Ceará, Brazil*

ARTICLE INFO

Article history:
Received 6 July 2019
Accepted 27 March 2020
Available online 16 April 2020

Keywords:
In-situ alloys
Welding
Tandem GMAW process

ABSTRACT

The present study discusses the use of the Tandem GMAW process as a technology capable of postponement manufacturing in the production of specific alloys, using different commercially available alloys. The results show that the Tandem GMAW process can be successful applied to produce *in-situ* alloys for specific purposes by combining different alloys during the welding procedure, leading to advances in the manufacturing and development of new alloys. Based on this technique it is possible to map the binary or multicomponent alloys with their new metallurgical features that are different from the original metals or alloys, which can be deposited in various different proportions. In addition, this technique allows the optimization in multicomponent alloy systems, by finding suitable combinations of chemical elements from commercial alloys, and thereby increasing the range of options for the industrial sector. Furthermore, the industrial use of this technique will increase the prospects of these complex alloys and consequently there will be a need to study the effects of the compositional modifications of these complex alloys as well as to evaluate the phase transformations and precipitation kinetics of these new alloys.

Metals and their alloys, such as steels and superalloys have enormous potential in science and engineering. This is due to the impressive combination of mechanical, physical and chemical properties that these metals and their alloys have [1,2]. Ni-based superalloys, for example, are a special class of materials due to their specific properties such as high-temperature strength, ductility, oxidation resistance, hot-corrosion resistance, and weldability [3–5].

In general, Ni-based alloys contain as many as 5–12 alloying elements that improve the mechanical properties and/or for the enhancement of corrosion and oxidation resistance [6].

---

[*] *Corresponding author.*
E-mail: cleiton@metalmat.ufc.br (C.C. Silva).

https://doi.org/10.1016/j.jmrt.2020.03.109

However, even with recent advances of the new generation of Ni-based alloys there are still many issue and applications which are unsolved. Such issues open up possibilities for the development of new alloys. As a general rule, when developing a new alloy, the concept and initial design are executed by computational methods, which help to guide the chemical elaboration and the procedures for melting and solidification. The next steps are the experimental procedures that include: fusion, liquid treatment, cleaning, solidification, heat treatments and mechanical processing. Consequently, the development of different kinds of alloys with a combination of different elements and metallurgical routes can be a challenging task.

Several methodologies have been proposed to study and manufacture bulk components. In the recent past, additive manufacturing emerged, and it has become an important materials processing technology [6–8]. Its enormous potential to build parts-on-demand using metals, ceramics, polymers or their combinations, with significant reduction of energy and cost, led to extraordinary advances in the field of materials science [9–11].

However, for applications involving pipelines as well as structures and heavy equipment, the most widespread manufacturing process is welding. Unfortunately, there are still many problems in the field of welding waiting for answers. One of these scientific and technological hot spots is dissimilar welding. A recent study highlighting some current challenges associated with fusion welding of materials for energy usages [12], cited dissimilar metal welds as a challenge for industrial applications. The risk of failure can be reduced by selecting the correct joint design and appropriate type of filler metal. Also, the dissimilarity, in many cases, is related to the deposition of a coating on a substrate. Many industrial applications require a corrosion resistant weld overlay. Stainless steels or nickel-based alloys are good options for corrosion protection with a low cost. However, in either case it is not always possible to select the best alloy for a specific application, due to several factors, including not being commercially available.

Therefore, the development of new alloys to assure specific features for specific applications is required for various industries. In the oil and gas, nuclear, energy, pulp and paper industries, among others, there is on-going research works on materials with improved performance for manufacturing equipment, as well as suitable materials for specific applications. Unfortunately, it is not always possible for the final customers of a supply chain to obtain exactly the ideal material for a given application. More expensive materials are used because of the absence of a commercial alloy with the desired characteristics. Thus, the development of a specific alloy, or the nearest possible, is indeed a necessity, and this could result in greater efficiency in the use of high-cost advanced materials. In basic welding with low-cost materials, it is common to choose commercial brands as filler metals that can serve a wide range of applications. However, for advanced applications using high-cost materials can become economically impracticable.

Some few studies are found in literature concerning the development of *in-situ* alloying by welding [13–15]. Ma et al. [16] combined gas tungsten arc welding (GTAW) process to produce *in-situ* alloying by separately depositing elemental pure Ti and pure Al wires. However, *in-situ* alloying development using two wires GMAW are not reported in the literature and opens new perspectives to this process. In addition, the studies developed until now are related to titanium aluminides, being *in-situ* Ni-based alloying development an unpublished subject matter.

Advances in welding processes have made improvements in arc stability and have increased deposition efficiency and productivity. One of the high productivity processes is the tandem gas metal arc welding (T-GMAW) process, which uses two wires [17–19]. Each wire has its own power source and they are insulated from each other in the welding gun.

The simultaneous use of different materials in this type of process results in the development of an *in-situ* alloy, that is different from either consumable when used individually as a filler metal. In these processes, each wire is equipped with a separate power supply, and gas shield device, and the welding process parameters can be adjusted individually to meet the various requirements of the desired weld. This new material has specific properties, which may differ by either the quantities of each wire used during the process or due to the process parameters such as the welding heat input, welding speed, and weaving, among others.

However, there is some difficulty to perform welds using this process, which is related to arc deflection. One of the possibilities to overcome it is the use of out-of-phase current pulse, aiming to give greater stability to the electric arcs. This is particularly important to allow the use of different filler metals with different proportions. Another aspect that is also widespread in pulsed GMAW welding is regarding metal transfer. The condition of a drop per pulse with droplet diameter close to the electrode has been sought aiming to make the process stable. However, in the T-GMAW configuration using electrodes with different feed speeds, it is not possible to maintain simultaneously the out-of-phase current pulse and the condition of one drop per pulse on both electrodes. Recent study showed that for welding made with T-GMAW process, applying different feed speeds, the use of out-of-phase current pulse became determinant for arc stability. It is also important for the quality of the weld bead itself with distinct droplet diameters between the two wires and larger than the diameter of the electrode [20]. Another point to consider is the wire speed limiting to perform a well-filled weld pool and result in a homogeneous weld on macro- and microscopic scale. This may limit the use of this technique to proportions within 30–70% of mixture.

Even though there is some complexity and limitations in using this process for *in-situ* welding production, the present study shows the use of the T-GMAW process as a technology for postponement manufacturing in the production of specific alloys, using different commercially available alloys. In this article, we will discuss some applications in which the production of *in-situ* alloys by the T-GMAW process was carried out successfully.

The first case is the production of an *in-situ* alloy using two different alloys as filler metal, shown in Fig. 1. In this example, a conventional low carbon steel (AWS A5.18 ER80S-D2), with a chemical composition of essentially Fe, with small amounts of silicon (Si), manganese (Mn) and carbon (C), was used as the filler metal. This metal essentially presents a ferritic microstructure with a body-centered cubic (BCC) crystal

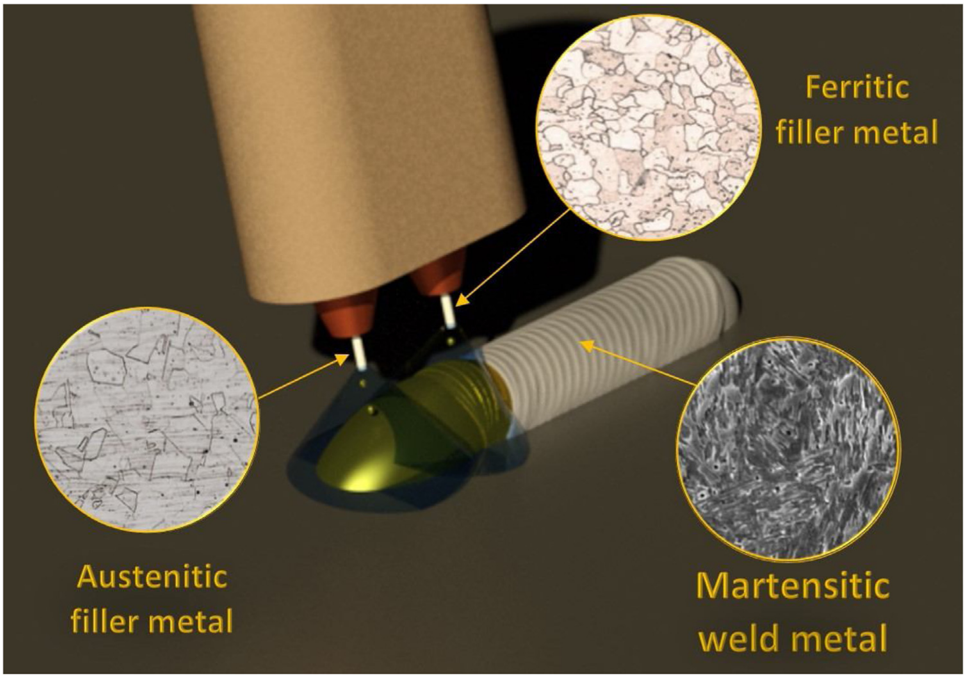

Fig. 1 – Drawing showing the Tandem GMAW torch and weld bead details during the welding. The differences in terms of microstructure of each wire for this specific application, and the microstructure in the weld fusion zone are also shown.

structure, which is a low cost commercial material. The other was an austenitic stainless steel (AWS A5.9 ER 307) wire containing Fe with additions of chromium (Cr), nickel (Ni) and manganese (Mn). The microstructure of this steel is essentially austenitic and it has a face-centered cubic (FCC) crystal structure. Although stainless steels are initially more expensive because of the additional alloying elements, specially nickel, they can become more accessible in price once the alloy is produced on a large scale and becomes widely available on the market.

The welds were performed using an x–y coordinate workbench and an IMC Digiplus A7 DCDU electronic power supply, which was developed for tandem MIG/MAG. All parameters of power and wire feed were monitored using a data acquisition system. The welding parameters and procedures used in this case were constant tension, resulting in a voltage of 18 V, a contact-tip-to-workpiece distance of 20 mm, and a welding speed of 10 mm/s, resulting in a heat input of 0.6 kJ/mm. The shielding gas was a mixture of 75% argon with 25% CO_2. The wire feed speed ranged from 4 to 6 m/min depending on the required weld pool chemistry.

In this example, the result was a novel *in-situ* alloy with high hardness and good mechanical properties, and which also presented a good corrosion resistance due to the participation of Cr and Mo as alloying elements in the weld metal. Different proportions of the alloys were tested within a specific range between 40 and 60 wt.% of each other. In this way different properties were achieved as a function of the ratios of each molten filler metal used. Microstructural analysis performed by optical microscopy (OM), indicated an apparently fully martensitic matrix, as shown in Fig. 2. This matrix is hierarchically structured in thin lath substructure, blocks, packet and grains (prior austenite grains) characteristic of low carbon high strength martensitic steels [21,22]. Additional analysis performed by scanning electron microscopy indicated also the presence of retained austenite along lath martensites, which can be attributed to the significant amount of austenitizing elements, especially Ni, from austenitic stainless steel. The chemical composition along the melted zone was very uniform (Fig. 2b), as was the microhardness. An example of two different filler metal proportions tested, which were evaluated for microhardness with a load of 0.1 kgf (0.98 N), resulted in 361.3 ± 3.7 and 452.5 ± 3.7 $HV_{0.1}$, showing a significant variability with low dispersion. These characteristics point to promising applications for industry, such as welding high strength steels, among others.

Another interesting application is the need for special materials that are used in oil and gas processing plant equipment, in nuclear energy plants as well as in the power generation and chemical industries to resist their specific corrosive environments. Various corrosion resistant alloys have been applied as a coating and are deposited by welding on low alloy steels or carbon steel. This leads to a significant reduction in costs when compared to the use of highly corrosive resistant steel in the first place. Depending on the application, alloys that offer the maximum resistance to corrosion, for example, can represent a high cost, making the process economically unviable. In other cases, it may be important to ally certain characteristics of an alloy with another having a different chemical composition and specific properties. The tandem gas metal arc welding (T-GMAW) process shows that it has ample flexibility from a metallurgical point of view to combine different alloys, resulting in an *in-situ* alloy, and therefore this method is able to guarantee the necessary characteristics required.

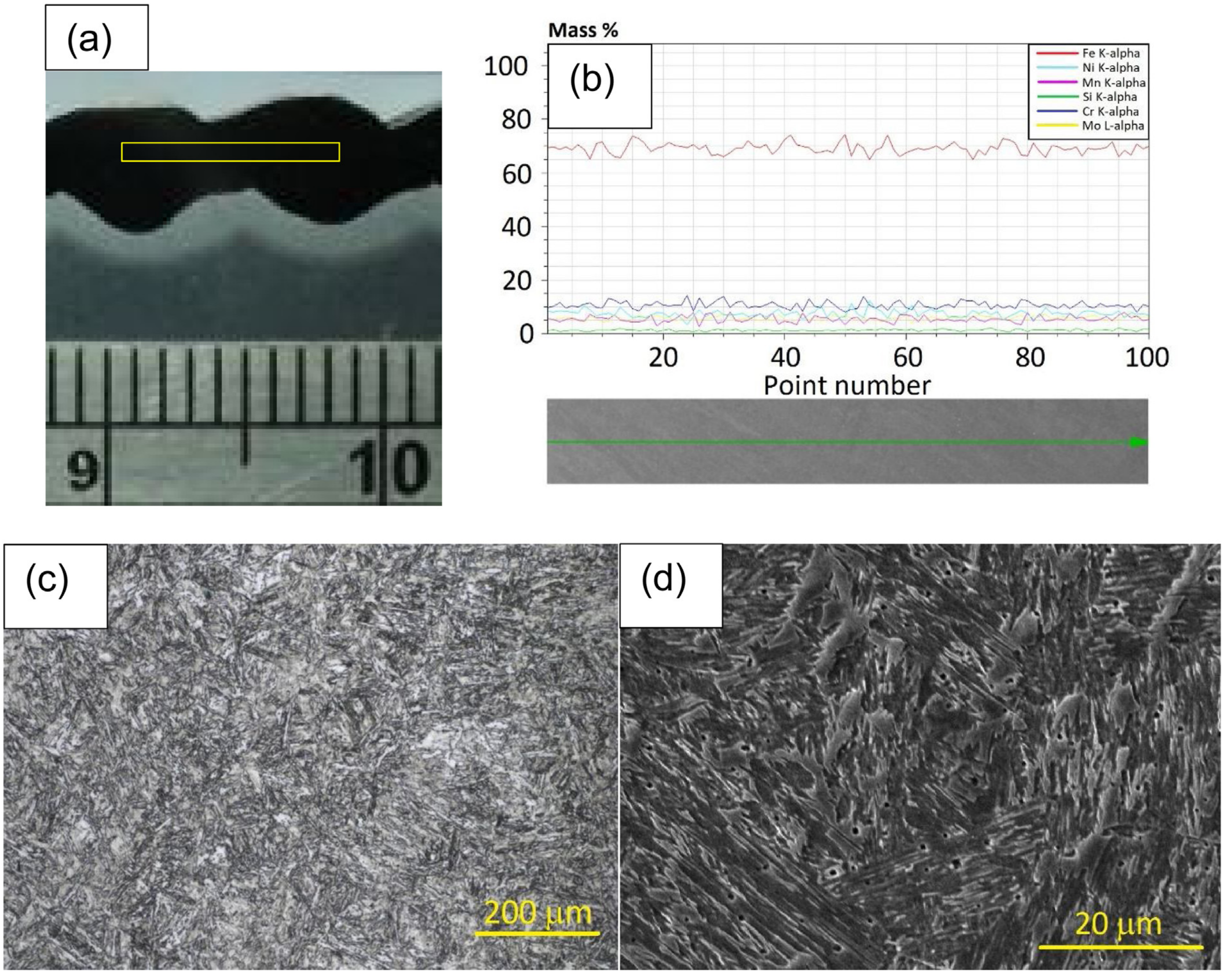

Fig. 2 – (a) Cross-section of weld overlay produced in-situ with using two different alloys as filler metal, a conventional low carbon AWS A5.18 ER80S-D2 steel with ferrite (bcc) and an AWS A5.9 ER 307 austenitic stainless steel (fcc) wire. (b) EDS linescan showing the resulting chemical composition, which was homogeneous along weld metal. (c) Light microscopy shown a martensitic matrix. (d) SEM analysis confirming the martensitic microstructure and some retained austenite between lath martensites.

A practical example is the use of nickel-based alloys as the internal coating of processing equipment and offshore steel pipelines. In general, the UNS N06625 alloy, with 20–22 wt.% of chromium, 9 wt.% of molybdenum, and an addition of niobium (4 wt.%) with iron limited to a maximum of 5 wt.% has been commonly used. In other situations, the UNS N10276 alloy, whose composition differs from the alloy 625 in terms of chromium (16 wt.%) and with higher percentages of molybdenum (16 wt.%), no niobium but with an addition of 4 wt.% of tungsten, can be used. In this case, chromium and molybdenum are essential for corrosion resistance. However, recent studies have shown that coatings deposited by welding using a third alloy, UNS N06686, obtained superior performance compared to previous ones [21,22]. The 686 alloy has the same chromium content as the UNS N06625 alloy (20–22 wt.%), with the same amount of molybdenum as the UNS N10276 alloy (16 wt.%), as well as tungsten additions (4 wt.%). However, its cost is higher when compared to the others.

This situation motivated an investigation into the performance of weld overlays produced by combining the UNS N06625 (AWS ER NiCrMo-3) and UNS N10276 (AWS ER NiCrMo-4) alloys, in order to create an *in-situ* novel alloy. Thus, an alloy with an intermediate composition between UNS N06625 and UNS N10276 alloys would be produced and which would approach the composition of the UNS N06686 alloy. The experimental procedure evaluating various welding parameters to obtain a stable arc with good metallic transfer, and which permitted the formation of a weld pool with a suitable contribution of each alloy.

In this case, the welds were performed in a KUKA KR16 robotic workbench and an IMC Digiplus A7 DCDU electronic power supply, developed for T-GMAW. All parameters of power and wire feed were monitored using a data acquisition system.

Some of the welding parameters selected to produce the novel Ni-based alloy based on the mixture of commercial alloys were kept constant: the contact tip to work distance was 20 mm and the welding speed was 20 mm/s. The operational mode was a constant pulsed current, with a peak current and a base current of 380 and 100 A, respectively. The heat input was 0.75 kJ/mm, and the shielding gas was 70% argon and 30%

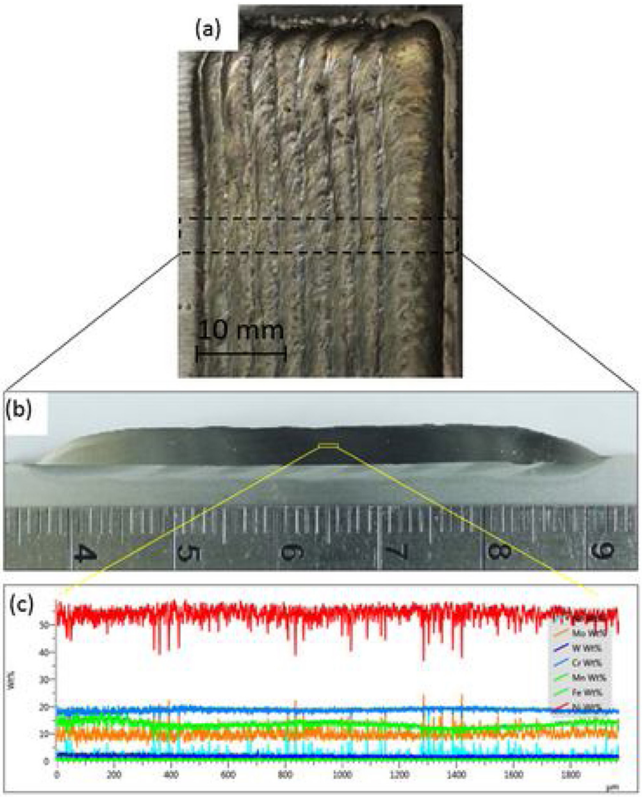

Fig. 3 – (a) Macrograph of the Ni novel alloy weld coating cross-section. (b) EDS linescan through several microns along the dashed-line shown in the macrograph.

He. More details on welding procedure and parameters can be found in recent publication [20].

Afterwards, several tests were carried out to evaluate the performance of the *in-situ* alloy. The final chemical composition was assessed by optical emission spectroscopy; the microstructural characteristics appraised by scanning electron microscopy (SEM), energy dispersive spectroscopy (EDS) and X-ray diffraction (XRD); also, corrosion resistance was evaluated by immersion tests according to the ASTM G48 standard.

The results showed that the use of this process for the production of *in-situ* alloys was feasible, since the welds were of good quality, without defects or cracks. The coatings produced showed good chemical and microstructural homogeneity. Energy dispersive of X-ray spectroscopy (EDS) linescan for the main elements confirmed the good quality of the deposits, as shown in Fig. 3. Microsegregation of some alloying elements such as Mo, Nb, and W occurred during solidification of the weld metal. These partitioning of alloying elements resulted in an enrichment of the aforementioned elements in small portions of liquid metal in the end of solidification.

This microsegregation resulted in the formation of secondary phases, which was another important feature evaluated. The microstructural analysis of *in-situ* alloy indicated the presence of two different secondary phase particles, being one with cuboidal morphology and rich in Nb, Ti, C and N. This is characteristic of TiN/NbC core/shell structure, similar to reported in previous study [23]. The second structure presented a misshapen morphology, characteristic of solidification of residual interdendritic liquid. Based on XRD and SEM-EDS analysis, these particles were identified as topologically closed packet phases rich in Mo, Nb and W, with rhombohedral crystal structure, known as μ-phase, similar to the reported in literature for other NiCrMo alloys [24]. Further investigations by TEM should be performed to elucidate the structure and chemistry in nano scale.

This microstructural pattern regarding to the secondary phases for the *in-situ* alloy is uncommon and interesting, being directly related to the microstructural feature of each commercial alloys. The microstructure of the UNS N06625 dissimilar weld was characterized by scanning electron microscopy (SEM), transmission electron microscopy (TEM) and X-ray diffraction (XRD) analysis. The microstructure consisted of a γ-fcc matrix with cuboidal particles formed by a core of titanium nitride (TiN) and a shell of niobium-titanium carbides (NbTiC), forming (TiN)/(NbTiC) complex precipitates, and a Nb-rich Laves phase [23,25], as shown in Fig. 4a. While the microstructure of the UNS N10276 dissimilar weld was formed by Mo-rich topologically-closed packed (TCP) phases (σ-, μ- and P-phases), precipitated in a γ-fcc matrix, as shown in Fig. 4b [24,26]. The results of the microstructure for the novel *in-situ* alloy showed that the (TiN)/(NbTiC) complex precipitates remained in the microstructure, since the TiN nitrides is in the solid state during the fusion, acting as a nucleating agent for the formation of the (NbTi)C carbide shells [23]. The combination of molybdenum, tungsten and niobium elements in the same alloy and its microsegregation behavior resulted in a local liquid chemical composition, at the end of the solidification process. This complex local chemical composition was able to suppress the Nb-rich Laves phase and Mo-rich σ-phase and P-phase. Thus, the secondary phases that resulted from the solidification of the *in-situ* alloy were (TiN)/(NbTiC) complex precipitates, as a direct contribution of the UNS N06625 alloy, and the μ-phase was the result of the blend of the molybdenum, tungsten and niobium. In that case, the molybdenum and tungsten were contributions from the UNS N10276 alloy whereas the niobium and molybdenum were contributions from the UNS N06625 alloy. The differences in terms of microstructure and microchemistry found in these studies will directly affect the properties of the alloys.

In this particular application, the *in-situ* alloy was designed to be used as a corrosion resistant alloy; therefore, it had to be evaluated from this point of view. Based on the results of the ASTM G48 tests, the performance of the *in-situ* alloy was superior to the UNS N06625 and UNS N10276 alloys separately, and comparable to the performance achieved by the UNS N06686 alloy [27,28]. This clearly demonstrates the feasibility of this technique not only for the development of experimental alloys for scientific use but also for practical applications in industry. Moreover, this process had a higher productivity, due to the welding speed of the T-GMAW process that has considerably higher welding speeds than conventional processes.

In summary, the tandem gas metal arc welding (T-GMAW) process can be successful applied to produce *in-situ* alloys for specific purpose. This goal was achieved by the combination of different alloys during the welding procedure, leading to advances in manufacturing and development of materials.

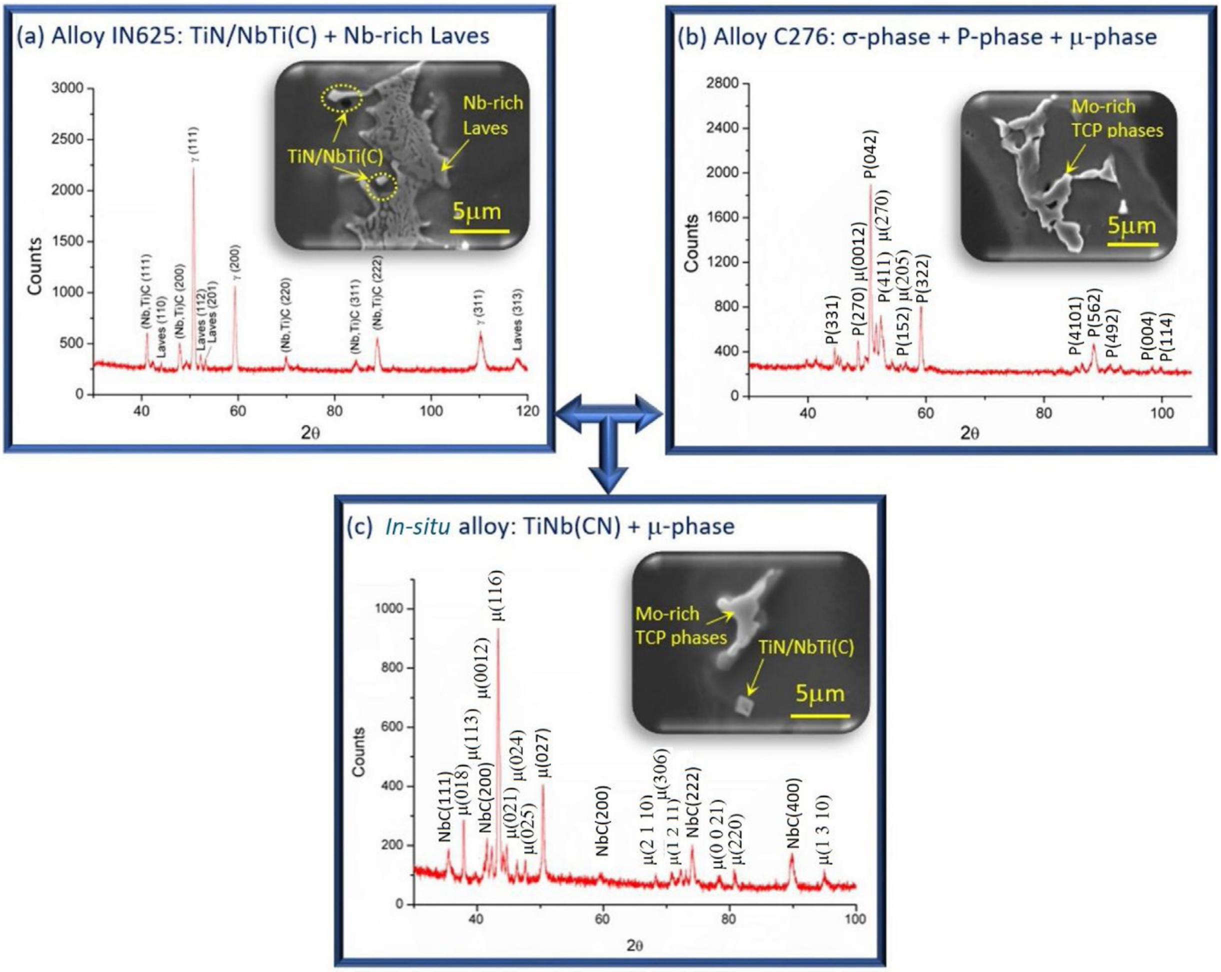

Fig. 4 – Exemples of some microstructural features of the novel Ni-based alloy produced from the IN625 and C276 alloys. (a) The X-ray diffraction spectrum of secondary phases extracted from UNS N06625 alloy displaying Nb-rich Laves phase and TiN/NbTi(C) nitrides/carbides with the respective SEM image showing both phases. (b) X-ray diffraction spectrum of secondary phases extracted from UNS N10276 alloy displaying peaks referring to the Mo-rich TCP phases such as P-, µ- and σ-phase with a SEM image showing an example of the Mo-rich particle. (c) Novel Ni-based alloy X-ray diffraction spectrum showing peaks indexed only for two secondary phases extracted from the matrixes: NbC from the UNS N06625 alloy and the µ-phase attributed to the UNS N10276 alloy. In addition, a SEM image is presented showing the NbC particle together with the Mo-rich phase.

Based on this technique it is possible to map binary or multicomponent alloys with metallurgical features different from their original metals or alloys using different proportions of filler metals. In addition, this technique allows optimization in multicomponent alloy systems, finding the most suitable combination of chemical elements from commercial alloys, and thus increasing the range of options for industry. Furthermore, the application of this technique will increase the prospects of these complex alloys. Consequently, there will be a need to study the effects of compositional modifications as well as to evaluate the phase transformations and precipitation kinetics of these new alloys.

Conflicts of interest

The authors declare no conflicts of interest.

Acknowledgements

The authors would like to thank the funding agencies FUNCAP and CAPES for financial support (Project AE1-0079-000490100/13) and CNPq for scholarship grants. Also, PETROBRAS for their collaboration in this project. The X-ray Laboratory and Analytical Center of the UFC, project CT-INFRA/MCTI-SISNANO/PRÓ-EQUIPAMENTOS CAPES.

Appendix A. Supplementary data

Supplementary material related to this article can be found, in the online version, at doi:https://doi.org/10.1016/j.jmrt.2020.03.109.

REFERENCES

[1] Lu K. The future of metals. Science 2010;328:319–20.
[2] Pollock TM. Alloy design for aircraft engines. Nat Mater 2016;15:809.
[3] Padture NP, Gell M, Jordan EH. Thermal barrier coatings for gas-turbine engine applications. Science 2002;296:280–4.
[4] Cormier J. Materials science: not so creepy under stress. Nature 2016;537:315–6.
[5] Darling KA, Rajagopalan M, Komarasamy M, Bhatia MA, Hornbuckle BC, Mishra RS, et al. Extreme creep resistance in a microstructurally stable nanocrystalline alloy. Nature 2016;537:378–81.
[6] Frazier WE. Metal additive manufacturing: a review. J Mater Eng Perform 2014;23:1917–28.
[7] Francois MM, Sun A, King WE, Henson NJ, Tourret D, Bronkhorst CA, et al. Modeling of additive manufacturing processes for metals: challenges and opportunities. Curr Opin Solid State Mater Sci 2017;21:198–206.
[8] Singha S, Ramakrishna S, Singh R. Material issues in additive manufacturing: a review. J Manuf Process 2017;25:185–200.
[9] Sames WJ, List FA, Pannala S, Dehoff RR, Babu SS. The metallurgy and processing science of metal additive manufacturing. Int Mater Rev 2016;61:315–60.
[10] Qin Z, Jung GS, Kang MJ, Buehler MJ. The mechanics and design of a lightweight three-dimensional graphene assembly. Sci Adv 2017;3:e1601536.
[11] Sweeney CB, Lackey BA, Pospisil MJ, Achee TC, Hicks VK, Moran AG, et al. Welding of 3D-printed carbon nanotube-polymer composites by locally induced microwave heating. Sci Adv 2017;3:e1700262.
[12] Dupont JN, Babu S, Liu S. Welding of materials for energy applications. Metall Mater Trans A 2013;44A:3385–410.
[13] Ueyama T, Ohnawa T, Tanaka M, Nakata K. Effects of torch configuration and welding current on weld bead formation in high speed tandem pulsed gas metal arc welding of steel sheets. Sci Technol Weld Join 2005;10(6):750–9.
[14] Li KH, Zhang YM. Consumable double-electrode GMAW-Part 1: the process. Weld J 2008;87:11.
[15] Li KH, Zhang YM. Consumable double-electrode GMAW part II: monitoring, modeling, and control. Weld J 2008;87:44.
[16] Ma Y, Cuiuri D, Hoye N, Li H, Pan Z. Characterization of in-situ alloyed and additively manufactured titanium aluminides. Metall Mater Trans B 2014;45:2299–303.
[17] Dong B, Pan Z, Shen C, Ma Y, Li H. Fabrication of copper-rich Cu-Al alloy using the wire-arc additive manufacturing process. Metall Mater Trans B 2017;48:3143–51.
[18] Geng H, Li J, Xiong J, Lin X, Zhang F. Optimization of wire feed for GTAW based additive manufacturing. J Mater Process Technol 2017;243:40–7.
[19] Ma Y, Cuiuri D, Shen C, Li H, Pan Z. Effect of interpass temperature on in-situ alloying and additive manufacturing of titanium aluminides using gas tungsten arc welding. Additive Manuf 2015;8:71–7.
[20] Santiago KG, Fernandes IP, Miranda HC, Silva CC, Motta MF. Influence of out-of phase current pulse in the T-GMAW pulsed process stability with different wire feed speeds. Weld Insp 2018;23:423.
[21] Morito S, Tanaka H, Konishi R, Furuhara T, Maki T. The morphology and crystallography of lath martensite in Fe-C alloys. Acta Mater 2003;51:1789–99.
[22] Morito S, Huang X, Furuhara T, Maki T, Hansen N. The morphology and crystallography of lath martensite in alloy steels. Acta Mater 2006;54:5323–31.
[23] Silva CC, Miranda HC, Motta MF, Farias JP, Afonso CRM, Ramirez AJ. New insight on the solidification path of an alloy 625 weld overlay. J Mater Res Technol 2013;2:228.
[24] Silva CC, Miranda HC, Motta MF, Farias JP, Afonso CRM, Ramirez AJ. Highlights 686. J Alloys Comp Technol 2013;2:228.
[25] Silva CC. PhD. Thesis. Brazil: Universidade Federal do Ceará; 2010.
[26] Aguiar WM. PhD thesis. Brazil: Universidade Federal do Ceará; 2010.
[27] Pessoa EF. PhD. Thesis. Brazil: Universidade Federal do Ceará; 2014.
[28] Silva CC, Afonso CRM, Ramirez AJ, Motta MF, et al. Evaluation of the corrosion resistant weld cladding deposited by the TIG cold wire feed process. Mater Sci Forum 2014;783–786:2822–7.